High intensity illumination effects in $LiNbO_3$ and $KTiOPO_4$ waveguides

D. Eger, M. A. Arbore, and M. M. Fejer
Ginzton Laboratory, Stanford University, Stanford, California 94305-4085

M. L. Bortz
New Focus Incorporated, 2630 Walsh Avenue, Santa Clara, California 95051-0905

(Received 20 November 1996; accepted for publication 16 April 1997)

Quasi-phase-matched waveguides are known to degrade when generating high intensity short wavelength light. Photoinduced changes in the refractive indices can lead to reduced efficiency by broadening phase-matching curves or inducing power dependent losses. In this work a pump-probe technique was used to investigate photorefractive effects in nonlinear optical waveguides. A strong two photon photorefractive effect in single domain and Ti-poled $LiNbO_3$ was found that is considerably reduced in electric field periodically poled $LiNbO_3$ and is absent in Rb-exchanged $KTiOPO_4$. © *1997 American Institute of Physics.* [S0021-8979(97)03914-5]

I. INTRODUCTION

Optical waveguides of ferroelectric crystals such as $LiNbO_3$(LN) and $KTiOPO_4$(KTP) have import applications in the fields of optical communication, reprographics, and medical instrumentation. Of particular interest are the quasi-phased-matched (QPM) waveguides developed for doubling of diode laser light to generate coherent blue and laser light.[1] For LN these are made on periodically poled substrates by the annealed-proton-exchange (APE) method.[2] Rb-ion exchange is used for waveguide formation in KTP.[3] In spite of the large demand for short wavelength laser sources these devices have not yet reached the market. One of the main problems with such waveguides, which are required to operate at relatively high optical intensities and short wavelengths, is degradation in their performances with time.[4,5] This effect is complex because it involves several beams of different wavelengths and variable intensities propagating in the waveguide.

The main cause for optical damage in bulk LN is the photorefractive (PR) effect. This effect is reasonably well understood for low laser intensities up to 1 W/cm^2.[6] Light absorbed by an impurity center such as Fe^{3+} ion generates a free carrier into the conduction or valence band increasing the conductivity (σ). Due to the noncentrosymmetric structure of these materials a photovoltaic current (J) is generated and consequently an electric field is formed which modifies the refractive index via the linear electro-optic effect. Since they are created by the same one-photon excitation process, both the photovoltaic current and the photoconductivity scale linearly with the light intensity.[7] Thus the steady state electric field E_s, which is given in a one dimensional open circuit geometry by the ratio $-J/\sigma$, approaches a constant value independent of light intensity or absorption coefficient. To account for some deviations from this simple one-center one photon model, observed mostly at high illumination intensities, two center[7–9] or even three center[10] models have been suggested. Similar models have been also used to explain photosensitization of infrared holographic gratings by green light uniform illumination.[8]

There is only a limited amount of information in the literature on photoinduced damage mechanism in single domain waveguides of LN. Fujiwara *et al.*[11] have investigated the photorefractive effect induced by 633–1100 nm irradiation in Ti-diffused LN and 488 nm radiation in APE LN with light intensities up to 1 kW/cm^2.[12] They showed that their results for APE waveguides are consistent with the one-center model. Göring *et al.*[13] have investigated the photorefractive properties of planar APE LN up to 2 kW/cm^2 of 488 nm-light They found a linear photovoltaic current and a sublinear photoconductivity. Kondo *et al.*[14] used the photorefractive-grating method to compare the sensitivity to photorefractive damage induced by Ar laser illumination in different planar waveguides of LN and KTP.

In principle, a periodically poled structure is more resistant to PR damage than a single-domain one. The direction of the photovoltaic current is determined by the crystal polarity, which alternates in such a structure creating a grid of negative and positive charge. A significant part of the charge is annihilated by the lateral current flowing across the domain walls. The effect of the improvement of the resistance to PR damage in periodically poled LN has been reported in several recent papers[15–17] and modeled quantitatively by Taya *et al.*[18] To the best of our knowledge no reports are given in the literature on the PR effect in periodically poled LN waveguides.

The main motivation for our study was to determine the basic process responsible for the optical damage in QPM waveguides generating short wavelength light. An experimental method has been developed to characterize directly the photorefractive properties of different waveguides induced by the infrared light or by simultaneous launching of infrared together with blue light into the waveguide. The IR wavelength range used in this study was 700–900 nm with intensities up to 80 kW/cm^2, which are by at least an order of magnitude higher than those used in previous reports in the literature, but typical to the power densities in operational QPM devices. In this article we present the results of a comparative study of the PR effect in APE single domain and periodically poled LN waveguides. Also shown are results on Rb-exchanged KTP. It is concluded that the photovoltaic current is determined by a two-photon effect. Our results indicate that the sensitivity to PR damage is considerably reduced in EF-poled LN as compared to single domain or

 0021-8979/97/82(3)/998/8/$10.00

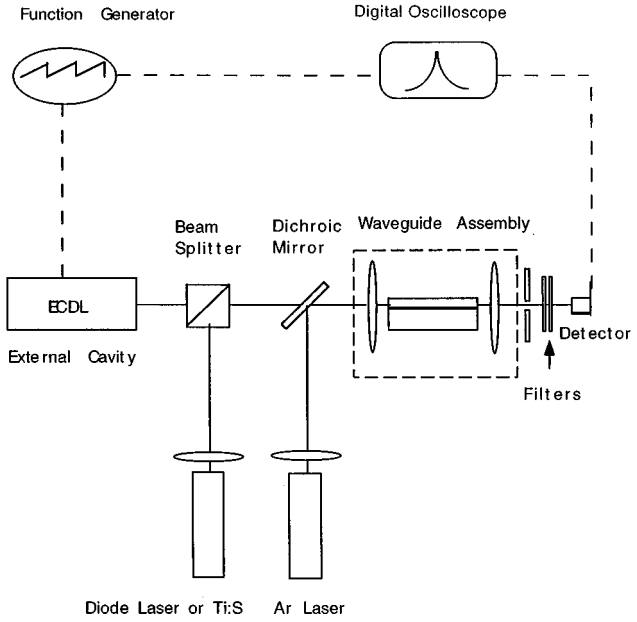

FIG. 1. Schematic diagram of the experimental setup.

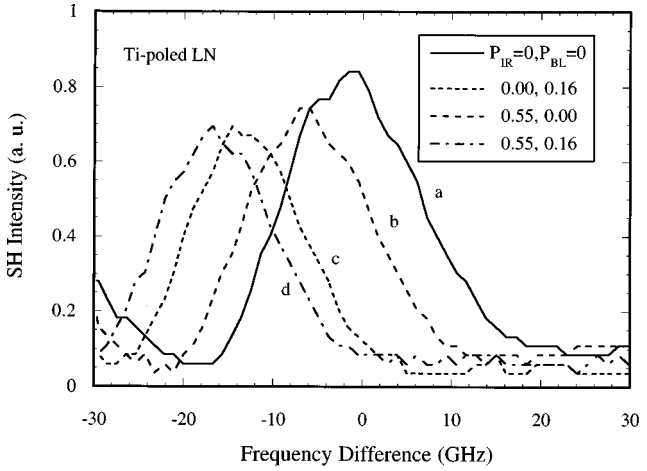

FIG. 2. QPM tuning curves of a Ti-poled LN waveguide for different pump powers coupled into the waveguide.

Ti-poled waveguides. No PR effects were observed in KTP waveguides.

II. EXPERIMENT

A. Measurement technique and data analysis

A pump-probe method was used in this work to investigate the photo-induced effects in different waveguides. The experimental setup is shown in Fig. 1. For the probe we used a tunable external cavity diode laser (ECDL) operating in the range of 770–790 nm and tunable up to 60 GHz. The IR pumps used here were a high power Fabry–Perot (FD) diode laser or a tunable Ti:S laser. For a visible light pump we used a multiaxial Ar laser operated at 514 or 488 nm lines. The different pump beams were coupled into the waveguide collinearly with the probe beam. All the beams were polarized along the z axis of the investigated wafers (p polarization). Basically we made four types of measurements with this system:

1. Fabry–Perot fringe shift

FP fringes are formed by the interference between the multiple reflections of the probe beam from the waveguide facets. In this measurement the probe beam was coupled into the waveguide by a mode matching lens and the transmitted intensity was detected by a Si photodiode. The fringe pattern trace, namely the intensity versus frequency, was displayed directly on the oscilloscope using a sawtooth modulation of the probe frequency. When the index of refraction was changed by coupling one of the pumps into the waveguide, the fringe pattern shifted relative to its original position. Since the relative change in the frequency is small, ($\delta f/f_{\mathrm{FP}} \ll 1$) the modal index change is given by:

$$\delta n_{\omega} = -n_{\omega}\delta f/f_{\mathrm{FP}}, \tag{1}$$

where f_{FP} is the FP frequency, δf is the shift in the frequency, and n_{ω} is the modal effective index of the waveguide. The sensitivity of the measurement was about 10^{-6} but the accuracy in the evaluation of the steady state index change was limited in some samples by slow drifts which induced variations up to 20%.

2. QPM tuning curve shift

This measurement was used for QPM waveguides generating UV light by selecting the central wavelength of the ECDL to be the phase matching one. In principle, the measurement was similar to that of the FP fringes except in their case the IR light was blocked by optical filters and only the generated UV light reached the detector. The sawtooth modulation of the probe frequency, while monitoring the intensity, allows an entire phase-matching curve, of typical 10–20 GHz to be displayed on the oscilloscope. An example of a family of such traces for different combinations of pump powers is shown in Fig. 2. As shown in the figure, when different pump beams are coupled into the waveguide the QPM curve shifts due to the changes in the modal indices induced by the optical power. The induced difference in the modal indices is given by:

$$\delta n_{2\omega} - \delta n_{\omega} = -(n_{2\omega} - n_{\omega})\,\delta f/f_{\mathrm{QPM}}, \tag{2}$$

where $n_{2\omega}$ is the effective modal index of the generated second harmonic (SH) light and f_{QPM} is the QPM frequency. The QPM curve shift measurement coupled with the FP fringe shift measurement allows one to determine the change in the SH modal index which cannot be done by the fringe technique alone. It should be noted that the intensity of the probe of about 5 kW/cm^2, which we had to use for this measurement to get sufficient SH power, was high enough to cause some frequency shifts. However since we were only interested in the changes induced by the pumps and not in the absolute values of the refractive indices, this shift was of no consequence to our measurement.

3. SH intensity decay

The measurements described above were done with cw pumps. However, important data on the time evolution of the photo-induced processes can be obtained from the response of different parameters to pulsed pumps. For these measurements we fixed the frequency of the probe close to the QPM wavelength and used an acousto-optic modulator for on-off modulation of the IR or of the blue light pump intensities. The pulses changed the phase-matching conditions inducing a decay in the SH intensity ($I_{2\omega}$) which was displayed on the oscilloscope. Usually, we used low repetition rate (1–10 Hz) and low duty factor (1:10) pulses to allow for the full recovery of the SH peak between the pulses. The parameter derived in these measurements was the initial decay slope defined as:

$$\tau \equiv -1/[I_{2\omega}(\partial I_{2\omega}/\partial t)_{t=0}]. \tag{3}$$

4. Beam throughput variations

In these measurements we have investigated the effect of the change in the transmission through the waveguide of one of the pumps or of the probe by coupling another pump into the waveguide.

To estimate some of the basic photorefractive properties of the waveguide we used the following relations:

$$\mathbf{E} = 2\,\delta n/(n^3 r_{33})\mathbf{e_z}, \tag{4}$$

where $\mathbf{E}$ is the photo-generated electric field, $\mathbf{e_z}$ is the unit vector in the $\mathbf{z}$ direction, r_{33} is the electro-optic coefficient, and n stands for the modal index of either the fundamental or the second harmonic wave,

$$\mathbf{E_s} = -\mathbf{J}/(\sigma_{\mathrm{PC}} + \sigma_d), \tag{5}$$

where $\mathbf{E_s}$ is the steady state electric field, σ_{PC} is the photoconductivity, σ_d is the dark conductivity, and the photovoltaic current is given by

$$\mathbf{J} = -\kappa \epsilon_O (\partial \mathbf{E}/\partial t)_{t=0}, \tag{6}$$

where κ is the dielectric constant, ϵ_O is the permitivity of the free space, and the field derivative is taken at the initial time when the pump is applied. These relations are valid for uniform illumination and assuming that the free carrier lifetime is much shorter than the electrical equilibrium time. The illumination of the samples in our experiments is clearly not uniform as the intensity of the beams vary across the waveguide with a Gaussian-like distribution. In this case the values of different physical quantities become dependent on the coordinates. However, it can be shown that in the case the concentration of the free carriers is proportional to the light intensity, the relations in Eqs. (4), (5), and (6) are still valid provided that the physical quantities, which have distributed values across the beam such as $\mathbf{E}$, $\mathbf{J}$, and σ_{PC}, are replaced by their values averaged over the light intensity.

B. Waveguide specifications and processing

The APE method was used to produce waveguides on single domain and periodically poled z-cut LN substrates. The protonation process was done in a benzoic acid bath at 178 °C for 0.5 h to a depth of 0.2 μm through a lithographically defined mask of sputtered SiO_2 with 3.5- and 4.0-μm-wide channel openings. The sample was annealed in air at 340 °C for 2.5 h. The waveguides were designed to support a single transversal mode at 780 nm. The substrate poling was done prior to the pling process by Ti diffusion or by using an electric field. Details of the Ti poling process are given in previous publications.[19,20] Basically, a 50-Å-thick Ti film was patterned by wet etching onto a grating with 2.1 μm period and 1.0 μm lines on the $+z$ surface of the $LiNbO_3$ substrate. The patterned substrate was covered with congruent LN powder and then heated up to 1100 °C in a closed Al_2O_3 crucible with a $2h$ linear ramp, soaked for 4 min, and cooled down at a rate of 8 °C/min. By this process a shallow triangular pattern of inverted domains is obtained of average depth comparable to the period length. The 1-cm-long waveguides prepared this way had a normalized efficiency of 100% $W^{-1}cm^{-2}$ at 780 nm and a tuning curve width of about 10 GHz.

The EF poling process used in this work was done using the liquid electrolyte contact method as described in detail by Myers *et al.*[17] and by Miller *et al.*[21] Due to the difficulty in forming short-pitch gratings by this method, the waveguides were designed with a 6.5 μm period for third order frequency doubling at 780 nm. Even for this period the structures were not perfect having missing patches and consider fluctuations in their duty factor. These samples showed broad SH tuning curves of over 100 GHz in their width, which severely reduced the accuracy of the QPM curve shift measurement. Some additional measurements were done on better quality 24 μm period EF-poled samples using the FP fringe technique.

The periodically poled KTP waveguides investigated in this work were produced by groups at Du-Pont and Soreq NRC using Rb-exchange processes on flux grown z-cut substrates. The substrates, patterned by a metallic mask on the z surface, were exchanged in a $RbNO_3$ bath for 30 min at 330 °C.[22] The period length was 2.8 μm designed for first order frequency doubling around 780 nm. The waveguide widths were 4–6 μm and length was 1 cm. The frequency doubling efficiencies were between 50% and 100% $W^{-1}cm^{-2}$. Some additional waveguides of longer periods were also investigated.

III. RESULTS

A. The effect of the IR irradiation

The change in the refractive indices of the Ti-poled sample induced by 1 mW IR pump [derived according to Eqs. (1) and (2)] is shown in Fig. 3. Both n_ω and $n_{2\omega}$ increase strongly as the pump wavelength is reduced. Also shown, the change in their difference which is much lower than the change in each of them individually. This change in the indices difference is responsible for the QPM curve shift.

Results of the steady state QPM frequency shift versus IR power measured at different wavelengths for a Ti-poled LN waveguide are shown in Fig. 4. As seen in the figure, for long wavelengths the absolute value of the shift is small and has a sublinear dependence on IR power. As the wavelength is reduced, the absolute value of the shift increases and the

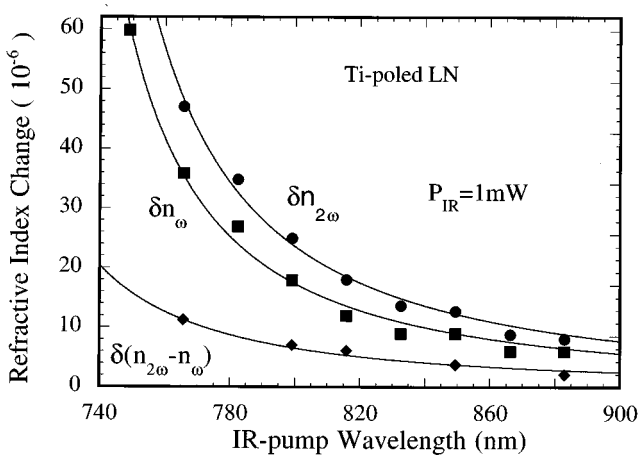

FIG. 3. Change induced by 1 mW IR pump in the second harmonic modal index, in the fundamental modal index and in the difference between them as a function of the wavelengths.

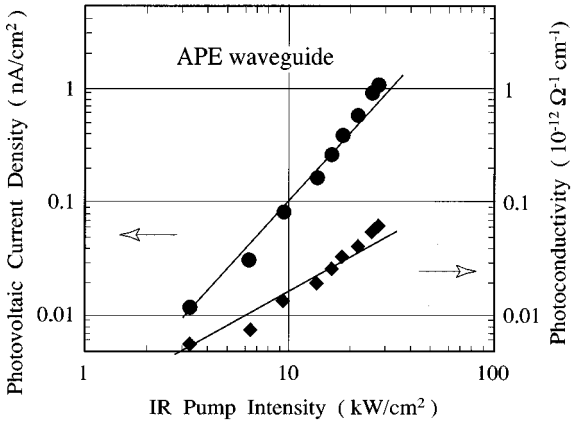

FIG. 5. Photovoltaic current density and photoconductivity as a function of IR pump intensity.

dependence on the IR power becomes linear. It should be noted that such linear scaling of the IR induced shift was observed for all of our LN samples whether periodically poled or having a single ferroelectric domain.

The photovoltaic current densities and photoconductivity values versus IR pump intensity, calculated by Eqs. (2), (3), and (4), for a single domain APE LN waveguide are shown in Fig. 5. Surprisingly, the photovoltaic current is a quadratic function of the IR intensity over two decades while the photoconductivity scales linearly with the pump intensity.

The refractive index change induced by 1 mW IR pump power for different samples is shown in Fig. 6. The most sensitive one is the single domain APE LN waveguide Ti poling seems to reduce the sensitivity, especially for long wavelengths. The sensitivity of EF-poled LN waveguides varied between the different samples but usually was lower than that of the single domain or Ti-poled LN waveguides. The effect of the IR pump on KTP waveguides is small and difficult to measure. The shift is in opposite direction to that of LN. For the KTP when the pump beam was directed into the substrate rather than into the waveguide a similar small frequency shift was observed, suggesting a thermal origin for the shift.

B. The effect of simultaneous coupling of IR and visible light

Coupling 488 nm Ar laser light into the waveguide in addition to the IR light reduced considerably the response time and increased the steady state index change. In Fig. 7 we show results of the steady state index change as a function of the 780 nm light power for various 488 nm light powers coupled into the Ti-poled waveguide. As seen, an approximate linear relation is observed between the index change and the IR power at fixed 488 nm power. The absolute value as well as the slope increase with the blue light power.

Figure 8 shows the SH intensity decay slope defined in Eq. (3) as a function of the power of the pump pulse taken for the Ti-poled sample. At low IR power we see a quadratic

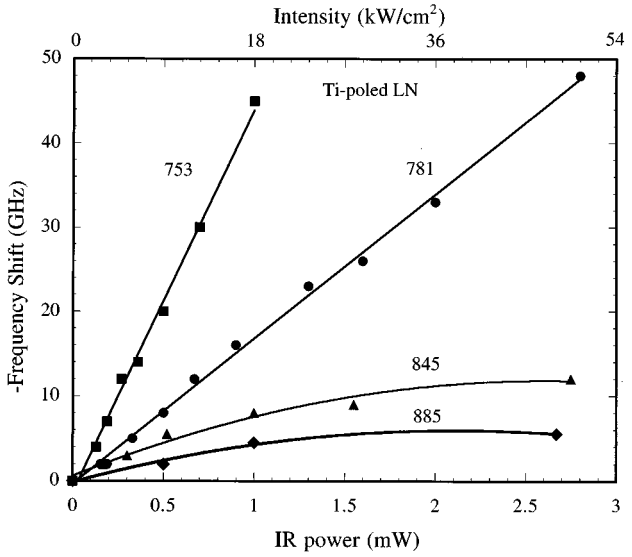

FIG. 4. Steady state frequency shift vs IR power for different wavelengths.

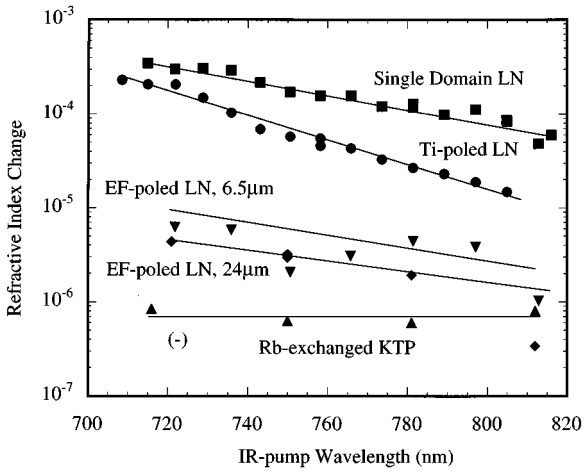

FIG. 6. Modal refractive index change induced by 1 mW IR pump as a function of wavelengths for different waveguides.

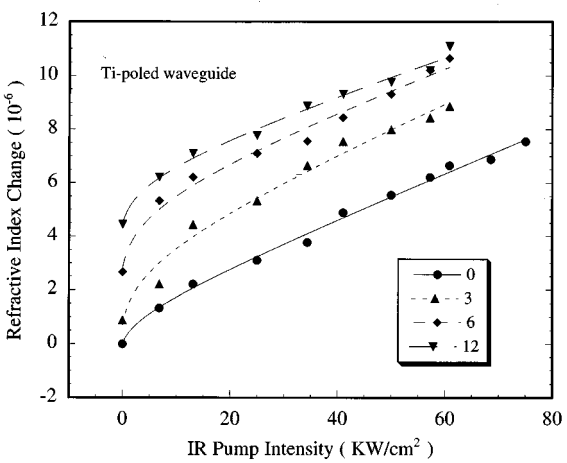

FIG. 7. Steady state modal index change as a function of IR pump intensity for different 488 nm pump intensities coupled into the waveguide.

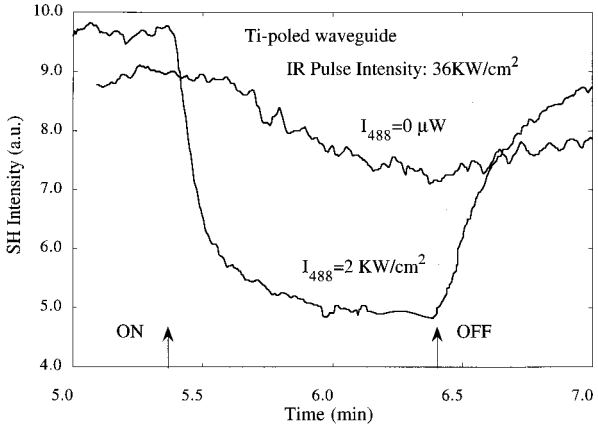

FIG. 9. SH intensity vs time during the application of an IR pulse.

dependence of the decay slope on the pump power similar to that observed for the single domain APE sample given in Fig. 5. Under these conditions, the decay slope is proportional to the photovoltaic current, thus this measurement provides an additional proof of the quadratic dependence of the photovoltaic current on the IR pump intensity for the different LN waveguides. At IR powers above 1 mW the results start to deviate from the quadratic dependence probably due to the broadening of the QPM tuning curve induced by the pump. For the 488 nm pump we see an approximate linear dependence represented by the solid line. It should be noted that in this case the blue light pump is coupled into the waveguide together with the IR probe and the results characterize the combined effect of the two waves.

The photosensitization of the effect induced by the IR light is demonstrated dramatically in Fig. 9. In this figure we show the effect of an IR pump pulse on the SH intensity generated by doubling the frequency of the probe. Initially the probe wavelength is selected at the SH curve peak. At the onset of the IR pump, the SH intensity starts to decay due to the shift in the quasi-phase-matching frequency. The decay caused by the IR pulse alone is slow and the recovery after the pulse termination is even slower. However when a relatively weak cw beam of 488 nm light is coupled into the waveguide the SH intensity decays much faster to a lower value. The recovery is much quicker too.

A similar effect obtained for the single domain APE LN waveguide is shown in Fig. 10. Here we applied a certain power of IR light and measured the shift in the fringe frequency with time. As seen, the rise time of the fringe shift curve is strongly enhanced by the low power blue light coupled into the waveguide approaching steady state values which increase with the blue light power as well

An additional interesting effect found in this study is the change in the throughput of a monochromatic beam induced by coupling a beam of another wavelength. An example of such an effect is shown in Fig. 11. In this experiment a 488 nm light beam emitted by the Ar laser was launched into the lowest order mode of the waveguide. Coupling of 2 mW of 780 nm light into the waveguide reduced the total throughput of the 488 nm light by about a factor of 2 and scattered the

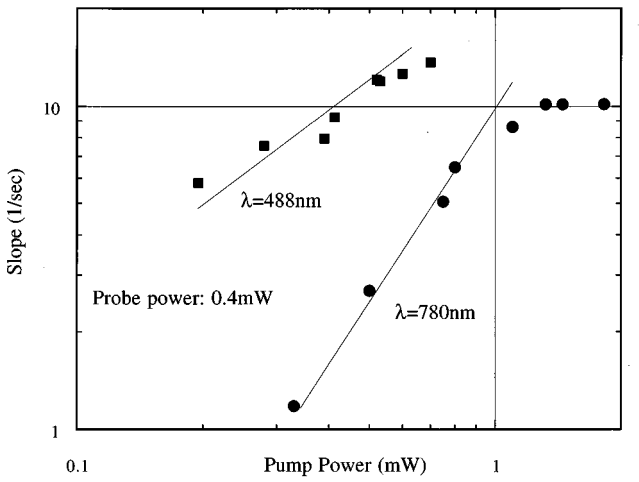

FIG. 8. SH intensity decay slope as a function of the power of the pump pulse.

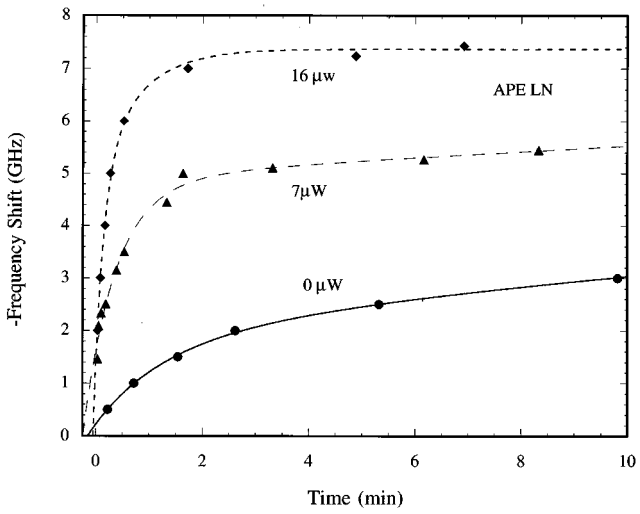

FIG. 10. FP fringe shift vs time for different powers of 488 nm pump coupled into the waveguide.

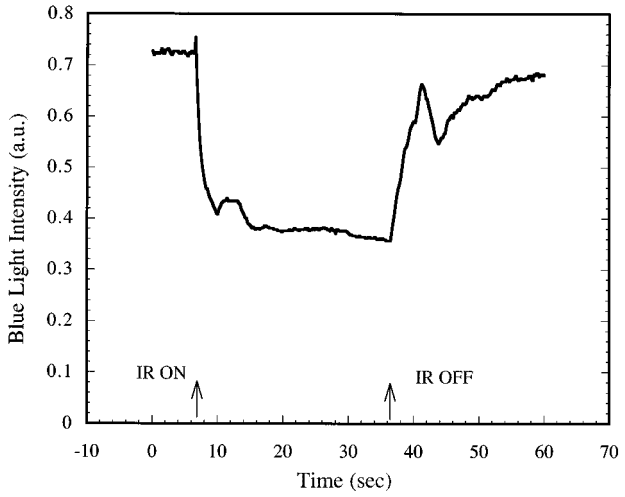

FIG. 11. Blue light intensity transmitted through the waveguide vs time.

blue light into several higher order modes. The throughput reduction was found to be caused by scattering of light out of the waveguide at low forward angles. While Ti-poled and single domain LN waveguides showed a more than 50% decrease in throughput, the effect was small for most of the EF-poled LN and not observable for KTP.

A reduction in IR throughput induced by the blue light pump was also observed in this work. This effect is smaller than the reverse one described above. Results are shown in Fig. 12. When the blue pump is coupled into a LN waveguide we usually see a quick drop in the transmitted IR power followed by a slow decay. The relative amount of the two vary between the different samples and depends on the optical alignment.

C. The effect of the blue light pump

In this work we were not able to separate the effect of the blue light pump from that induced by IR and from the combined IR and blue since we had to use an IR beam as a probe to take the measurements. However we got some indications on the relative intensity of the effects in LN waveguides from indirect measurements. Due to the low

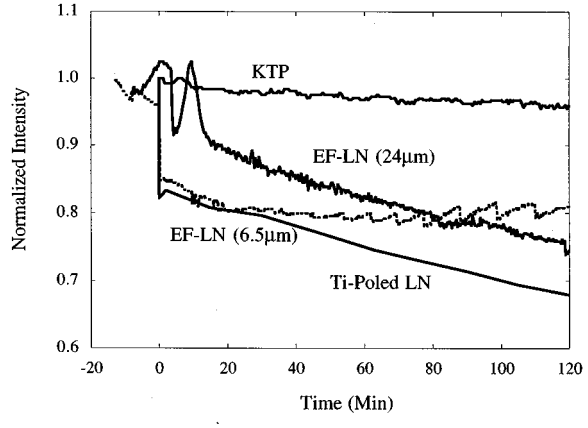

FIG. 12. IR light normalized intensity transmitted through the waveguide vs time for different waveguides.

dark conductivity, the changes induced by the IR beam in the indices of refraction persisted after blocking the light for several hours to days. Coupling only a few microwatts of blue light into the waveguide for a few seconds (after blocking the IR) were enough to erase the effects induced by the IR and to reset the system to its original position. This means that the blue light is highly efficient in generating photocarriers but not as efficient in generating a photovoltaic current.

IV. DISCUSSION

The one-photon excitation process base models used, usually to describe the photorefractive effect in bulk and APE LN waveguides, assume photovoltaic currents and photoconductivity which scales linearly with the irradiation intensity. In this case, at sufficiently high intensities (of about 1 W/cm^{-2}) the photoconductivity becomes much higher than the dark conductivity and the steady state induced electric field becomes saturated at a value independent of the pump intensity or wavelength. The results obtained in this work for the different LN waveguides do not agree well with these models: the photovoltaic current has a quadratic dependence on the IR light intensity and the electric field scales linearly with it in spite of the dark conductivity being negligible with respect to the photoconductivity. Moreover, the blue light beam coupled into the waveguide enhances strongly the index changes induced by the IR pump as opposed to the strong damping predicted by the one-photon models.

Our results can be explained schematically by assuming that the photovoltaic current is given by a second order expression while the photoconductivity is given by a first order expression of the pump intensities:

$$J = a_{11} I_{\mathrm{IR}}^2 + a_{12} I_{\mathrm{IR}} I_B \quad \text{and} \quad \sigma_{\mathrm{Ph}} = c_1 I_{\mathrm{IR}} + c_2 I_B . \tag{7}$$

The steady state electric field is given in this case by

$$E_s = -(a_{11} I_{\mathrm{IR}}^2 + a_{12} I_{\mathrm{IR}} I_B)/(c_1 I_{\mathrm{IR}} + c_2 I_B). \tag{8}$$

When only infrared light is coupled into the waveguide ($I_B = 0$) this expression gives a linear field with the IR intensity with a slope of $-a_{11}/c_1$. As the blue light becomes dominant, the electric field becomes again linearly dependent on I_B but with a slope of $-a_{12}/c_2$ which may be similar or different than the slope caused by the IR illumination alone. The expression in Eq. (8) can explain our results of the linear scaling of the frequency with IR intensity, the quadratic dependence of the photovoltaic current with the IR power, and the blue light induced photosensitization of the infrared effect.

The second order form of the expression for the photovoltaic current in Eq. (6) implies that it is the result of a two photon process. Similar dependence has been reported by von der Linde *et al.*[23] and was assigned to the intrinsic two photon absorption process. However in our case the IR photon energy is too low for direct interband two photon absorption. Probably, the excitation induced by the IR or the visible light interacts with another IR photon (or IR photon induced excitation) to generate photovoltaic current. An example for such a process is given in Fig. 13. We assume that APE waveguides of LN have two types of localized centers: an *A* center, which is normally occupied at room temperature,

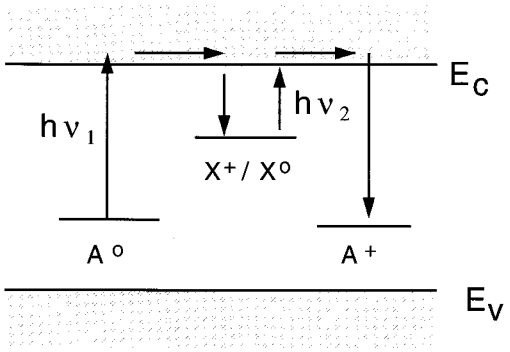

FIG. 13. Two photon process model.

and a more shallow X center which is normally empty. We further assume that the A center is not efficient in generating photovoltaic currents but the X center is highly efficient to do so. First an IR or blue photon absorbed at the A center generates an electron into the conduction band:

$$A^0 + h\nu_1 \rightarrow A^+ + e^-. \tag{9}$$

The photoconductivity depends mostly on this step of the process and therefore scales linearly with the intensity of the beam of ν_1 frequency. Then some small fraction of the electron are trapped at the X centers:

$$e^- + X^+ \rightarrow X^0. \tag{10}$$

A part of the trapped carriers are reemitted later into the conduction band by absorbing a second photon:

$$X^0 + h\nu_2 \rightarrow X^+ + e^-. \tag{11}$$

This step of the process generates the photovoltaic current which becomes dependent on the product of the two pumps intensities and of the IR beam intensity product with itself. The color centers may be defects introduced during waveguide fabrication such as A centers of oxygen vacancies and X centers of loosely bound polarons at Nb/Li antisites. Another possibility is that the A centers are Fe^{+2} impurities of the host crystal.

The strong dependence of the PR sensitivity on the IR pump wavelength observed for Ti-poled LN waveguides may be related to some hot electron effects. It is known that hot electrons can considerably increase the photovoltaic currents.[24] Another possibility is that this spectral dependence is a result of impurity band tailing.

The two color scattering effect observed in this work is probably related to the mixed term of the photovoltaic current. Usually the PR effect induces scattering because of its tendency to create and enhance optical nonuniformity. As the mixed term in the photovoltaic current increases the PR sensitivity also increases the mutual scattering of the two beams.

As mentioned in Sec. I, in principle, periodically poled structures are less affected by the PR effect than single domain ones. The EF-poled samples should be less sensitive than the Ti-poled ones due to their deep lamellar domain structure. This tendency was indeed observed in our measurements although the quality of the EF samples was not good enough to get a quantitative measure of the improvement.

Basically not one of the investigated KTP samples showed any PR effect. Yet Rb-exchanged waveguides made on flux grown KTP tend to degrade when generating short wavelength light. It is possible that the threshold intensity for photoinduced damage in KTP is higher than that used by us in this work or it requires shorter wavelengths. Our results indicate that the damage mechanism in KTP waveguides is different than that for LN.

V. SUMMARY

In this work we have shown that the pump probe system based on a tunable external cavity laser is a powerful tool for investigating photoinduced effects in nonlinear optical waveguides by measuring the shift induced by different pumps in the QPM tuning curve and in the FP fringe patterns we were able to determine the changes induced in the refractive indices and to evaluate the PR parameters such as the induced electric fields, photovoltaic currents, and photoconductivity.

The most sensitive sample to PR damage was found to be the single domain APE LN High sensitivity at short wavelengths was found for Ti-poled samples and a strong reduction in the sensitivity was found for EF-poled LN waveguides. No significant PR effects were found for KTP waveguides. The results obtained for the LN samples were not consistent with a one-photon excitation process but can be explained assuming a two-photon, two-center excitation process. Further work is required to identify the impurity centers responsible for these effects.

[1] Wezhi Wang, M. M. Fejer, R. H. Hammond, C. H. Ahn, M. L. Bortz, and T. Day, Appl. Phys. Lett. **68**, 729 (1996).
[2] J. K. Jakel, C. E. Rice, and J. J. Veselka, Appl. Phys. Lett. **41**, 607 (1982).
[3] J. D. Bierlein, L. H. Brixner, and S. Colak, Appl. Phys. Lett. **57**, 2074 (1990).
[4] M. L. Bortz (unpublished results).
[5] M. J. Jongeirous, R. J. Bolt, and N. A. Sweep, J. Appl. Phys. **75**, 3316 (1994).
[6] B. I. Sturman and V. M. Fridkin, *The Photovoltaic and Photorefractive Effects in Noncetrosymetric Materials*, edited by G. W. Taylor (Gordon and Breach Science, Philadelphia, PA, 1992), p. 19.
[7] G. A. Brost, R. A. Motes, and J. R. Rotge, J. Opt. Soc. Am. **5**, 1879 (1998).
[8] Erdeman, Opt. Commun. **93**, 44 (1992).
[9] K. Buse and E. Krätzig, Appl. Phys. B **61**, 24 (1995).
[10] K. Buse, F. Jermann, and E. Krätzig, Opt. Commun. **85**, 183 (1991).
[11] T. Fujiwara, S. Sato, and H. Mori, Appl. Phys. Lett. **54**, 975 (1989).
[12] T. Fujiwara, X. Cao, R. Srivastava, and R. V. Ramaswamy, Appl. Phys. Lett. **61**, 743 (1992).
[13] R. Göring, Zhan Yuan-Ling, and St. Steinberg, Appl. Phys. A **55**, 55 (1992).
[14] Y. Kondo, S. Miyaguchi, A. Onoe, and Y. Fujii, Appl. Opt. **33**, 3348 (1994).
[15] Y. L. Li, L. Mao, and N. B. Ming, Appl. Phys. Lett. **64**, 3092 ().
[16] V. Pruneri, P. G. Kazanski, L. Webjörn, P. St. J. Russel, and D. C. Hanna, Appl. Phys. Lett. **67**, 1957 (1995).
[17] L. E. Myers, R. C. Eckkart, M. M. Fejer, R. L. Byer, W. R. Bosenberg, and J. R. Pierce, J. Opt. Soc. Am. B **12**, 2102 (1995).
[18] M. Taya, M. C. Bashaw, and M. M. Fejer, Opt. Lett. **21**, 857 (1996).

[19] M. L. Bortz, S. J. Field, M. M. Fejer, D. W. Nam, R. G. Waarts, and D. F. Welch, IEEE Trans. Quantum Electron. **30**, 2953 (1994).
[20] E. J. Lim, M. M. Fejer, R. L. Beyer, and W. J. Kozlovsky, Electron. Lett. **25**, 731 (1989).
[21] G. D. Miller, R. G. Batcho, M. M. Fejer, and R. I. Beyer, in *SPIE Proceedings on Nonlinear Frequency Generation and Conversion, 2700* (SPIE, Bellingham, WA 1996), p. 34.
[22] D. Eger, M. Oron, M. Katz, and A. Zussman, J. Appl. Phys. **77**, 2205 (1995).
[23] D. von der Linde, M. Glass, and K. F. Rodgers, Appl. Phys. Lett. **24**, 155 (1974).
[24] B. I. Sturman and V. M. Fridkin, in *The Photovoltaic and Photorefractive Effects in Noncetrosymetric Materials*, edited by G. W. Taylor (Gordon and Breach Science, Philadelphia, PA, 1992).